



Competition of time and spatial scales in polymer glassy dynamics: Rejuvenation and confinement effects

Alexey V. Lyulin^{a,*}, Dmitri Hudzinskyy^{a,b}, Eric Janiaud^{b,c}, Antoine Chateauminois^c

^a Group Theory of Polymers and Soft Matter, Technische Universiteit Eindhoven, P.O. Box 513, 5600 MB Eindhoven, The Netherlands

^b Dutch Polymer Institute, P.O. Box 902, 5600 AX Eindhoven, The Netherlands

^c Laboratoire PPMD-SIMM, UPMC, CNRS UMR 7615, Ecole Supérieure de Physique et Chimie Industrielles (ESPCI), 10, rue Vauquelin, 75231 Paris Cedex 05, France

ARTICLE INFO

Article history:

Received 26 February 2010

Received in revised form 2 August 2010

Available online 31 August 2010

Keywords:

Glass transition;

Polymer rejuvenation;

Computer simulation;

Thin film

ABSTRACT

We use molecular-dynamics (MD) simulations and an original lateral contact experiment to explore the influence of mechanical history on polymer mechanical behavior and segmental mobility. Two typical glassy polymers are considered: bulk acrylate (experiments) and atactic polystyrene (aPS) in a bulk and in thin films (simulations). Stress-strain behavior has been investigated both experimentally for sheared, 50 μm thick, acrylate films and by MD simulations of an aPS in a bulk for two different strain rates in a closed extension–recompression loops. Cyclic shear strains applied in the plastic regime were found experimentally to induce a progressive transition of the mechanical response of the polymer glass toward a steady state which is characterized by a strong reduction of the apparent – non linear – shear modulus. The dynamics of the polymer glass in this yielded state was subsequently analyzed from a measurement of the time dependent linear viscoelastic properties at various imposed frequencies. Immediately after the cyclic plastic deformation, mechanical “rejuvenation” of the polymer is evidenced by a drop in the storage modulus and an increase in the loss modulus, as compared to the initial values recorded before plastic deformation. A progressive recovery of the viscoelastic properties is also measured as a function of time as a result of the enhanced aging rate of the system. This experimentally observed mechanical rejuvenation of polymer has been for the first time connected to the drastic increase in the simulated segmental mobility. A simulated distribution of relaxation times shows a shift to shorter times of the α and β relaxation processes which is consistent with the observed experimental changes in the viscoelastic modulus after rejuvenation. Finally, we present our first findings on the thickness- and substrate-dependence of the simulated glass transition temperature for thin aPS films. We observe the decrease of the glass transition temperature with film thickness, but for extremely thin (less than 2 nm) films.

© 2010 Elsevier B.V. All rights reserved.

1. Introduction

Polymer glasses are characterized by very broad spectrum of relaxation times. Polymer segmental mobility characterized by this spectrum (and polymer mechanical properties) is influenced by many factors, as physical aging, external mechanical deformation, spatial nanoconfinement, and many others. The main goal of the present study is to shed light on the influence of some of these factors on polymer segmental dynamics and its mechanical behavior.

Polymer glasses age with time. The concept of the physical aging of polymer materials was introduced by Struik long ago [1]. At that time Struik suggested that the large deformations in glassy polymers influence the physical aging process, mainly by creating the additional free volume. Since aging is supposed to occur due to some relaxation (decrease) in free volume, the free volume created by the deformation erases some part of the aging, and rejuvenation takes place. McKenna recently [2] showed

that after the application of deformation the polymer glasses end up into a new thermodynamic state which is different from that after thermal rejuvenation above T_g , meaning that some amorphous–amorphous transition takes place. This suggestion is supported by the concept of the potential energy landscape of the glassy state [3].

Jang and Jo [4] were among the first who performed the atomistic MD modeling for poly(trimethylene terephthalate), PTT, in a closed extension–compression deformation loop. They noticed that upon application of stress the distribution of polymer dihedral angles and polymer bond orientations is different in compression and under extension. By means of PALS experiments Cangialosi et al. [5] showed recently that plastic deformation (induced by a so-called “cold rolling” loading) applied to well-aged atactic polystyrene, aPS, and (bis)phenol-A polycarbonate, PC, samples lead to an increase in the size of the free-volume holes and a decrease of the holes concentration. Density measurements on cold drawn polycarbonate, acrylonitrile-butadiene-styrene (ABS) and PVC [6,7], and polystyrene [8] suggest some small (one–two percent) density increase after rolling instead of the expected (for the rejuvenated polymer) decrease. This effect is principally different from the physical aging after thermal rejuvenation which produces a

* Corresponding author.

E-mail address: a.v.lyulin@tue.nl (A.V. Lyulin).

reduction of the free-volume holes concentration and decrease of the density. These results on post-yield stimulated glasses suggest that mechanically rejuvenated polymers should have a structure qualitatively different from that of the thermally rejuvenated samples.

From Differential Scanning Calorimetry (DSC) measurements on stretched glassy polymers, Hasan and Boyce [9] concluded that the rearrangements associated with inelastic deformation act to store energy locally. Some insights into the associated rearrangements were recently provided from elastic neutron scattering of cold drawn acrylates [10]. These authors showed that the plastic deformation is homogeneous and is affine at scales larger than about half the entanglement distance. However, at length scales about the monomer size, the structure of the stretched polymer chains remains nearly isotropic but appears also slightly distorted by the plastic deformation. Recently, Lee et al. also probed experimentally the segmental dynamics of a polymer glass (PMMA) using an optical photobleaching technique [11]. They showed that segmental mobility increased by order of magnitudes upon the application of the tensile creep.

Computer-simulation studies of the changes in polymer dynamics under the influence of the deformation have been scarce. Capaldi et al. [12] showed the increased conformational transition rate upon the application of the uniaxial compression in MD simulations of a polyethylene-like chain. Using direct atomistic simulations of PC glass Lyulin et al. also showed [13] that the partitioning of the internal energy is completely different for thermally and mechanically rejuvenated polymers: the thermal rejuvenation is for more than 80% due to weaker van der Waals interactions, while the difference after a mechanical rejuvenation is for about 40% due to increased torsion of the PC chains. It was also shown that this different partitioning could be the main reason for the enhanced dynamics for the polymer rejuvenated samples. These results are supported by the recent MD simulations of Riggleman et al. [14,15] who observed the acceleration of the segmental dynamics under deformation and corresponding changes in the potential energy landscape. Warren and Rottler showed recently [16] that both dynamics and mechanical shift factors change by the same relative amount with aging time and applied stress.

On top of the dynamic temporal mechanical external stimulus, the effect of the polymer spatial confinement in a thin film of few tens nanometers thickness on its mechanical properties can be significant as well. Monte Carlo and MD computer simulations of Van Workum and de Pablo [17] showed that for confined polymers at a specified temperature the elastic modulus can be significantly smaller than that of a bulk material. Many experiments and simulations show that the glass transition itself is very different in thin polymer films and in a bulk. In the existing literature it is basically shown that the presence of the supported surface and the free interface drastically change both the static and dynamic behavior of the confined polymer chains.

In the present manuscript our aim is to understand how these external stimuli, like mechanical deformation or spatial confinement influence the glass transition in polymers in general, and aging phenomenon and its dynamics in particular, by doing both atomistic modeling and mechanical experiments on typical polymer glass formers. Cyclic shear experiments in the plastic regime have been carried out using a lateral contact method where a crosslinked glassy acrylate film is cyclically sheared within a contact between two elastic (glass) substrates [18]. As compared to more conventional mechanical experiments using bulk polymer specimens, this contact method presents the advantage of preventing the formation of macroscopic defects such as cracks within the glassy polymer when large strain cyclic strains are applied. We chose to apply a cyclic deformation instead of a monotonic loading because, after a given number of cycles, the glass reaches a steady state. Moreover, the application of a cyclic strain enables us to control the time scale of the mechanical stimulus through its frequency. Induced changes in the dynamics of the mechanically rejuvenated glass are monitored from a measurement of the linear viscoelastic properties after the application of the cyclic

plastic deformation. From such experiments we expect to get some insights into the changes in the relaxation time distribution of a yielded polymer glass.

Atactic polystyrene, aPS, is chosen for molecular-dynamics simulations. We would like to understand how the mechanical rejuvenation influences the whole spectrum of segmental relaxation times in a polymer glass. For this purpose not only some dynamical autocorrelation functions are simulated, but the whole distribution function of polymer relaxation times is calculated as well, for both non-rejuvenated and rejuvenated samples. Although the simulated aPS glass is different from the acrylate system used for experiments, qualitative comparisons between MD simulations and experiments can be envisaged out if one consider that the investigated mechanical rejuvenation processes are generic of many polymer glasses. We also would like to understand the influence of the confinement on the polymer glassy state itself. The glass transition in the ultrathin aPS films has been simulated for the first time.

The paper is organized as follows. The minimal details of the simulated model, used force field and implemented algorithms are explained in Section 2. Details of the performed experiments are introduced in Section 3. Section 4 studies the effects of simulated mechanical rejuvenation, and Section 5 contains the results of the cyclic shear experiments. Section 6 is devoted to the simulated spatial confinement effects. Finally, Sections 7 and 8 ends the manuscript with some discussion and conclusions.

2. Algorithm and simulation details

The united-atom representation of aPS is chosen for the MD simulations, no explicit hydrogen atoms are present, Fig. 1. The aPS model is described in detail by Lyulin et al. [19]. In short, the *NPT* MD simulations have been performed for 8 aPS polymer chains consisting of $N_p = 80$ monomers each (molecular weight ≈ 8300 Da, below one entanglement length) and its periodic images. The stereochemical configurations of the aromatic groups were generated at random so that the ratio of the number of *meso* to *racemic* dyads was near unity. We have also performed simulations for supported aPS films of different thicknesses in order to investigate the effects of the spatial confinement on a glass transition. Each film consists of 4, 8, 16, or 32 aPS chains (2564, 5128, 10256, 20512 united atoms, correspondingly). The average gyration radius of these chains is about $15 \text{ \AA} \div 20 \text{ \AA}$, which is comparable or below the film thickness in the simulated temperature range, 300 K–540 K. The monomer unit, Fig. 1, consists of two backbone ($-\text{CH}-\text{CH}_2-$) united atoms and the phenyl ring (the aromatic side group attached to the backbone).

All the interactions between aPS united atoms both in a bulk and in films are given by the following potential:

$$U_{PS} = \sum_{i,j} \varepsilon_{ij} \left[\left(\frac{\sigma_{ij}}{r_{ij}} \right)^{12} - 2 \left(\frac{\sigma_{ij}}{r_{ij}} \right)^6 \right] + \sum_{i,j} k_{l,ij} (r_{ij} - l_{ij})^2 + \sum_{i,j,k} k_{\theta,ijk} (\theta_{ijk} - \theta_{0,ijk})^2 + \sum_{i,j,k,l} k_{\phi,ijkl} \cos(n\phi_{ijkl}) \quad (1)$$

The force field U_{PS} includes non-bonded Lennard-Jones (LJ) interactions ($\sim \varepsilon_{ij}$) between united atoms which are on different chains or separated by more than three covalent bonds ($\varepsilon_{ij} \sim 0.1$ kcal/mol); a stretching potential ($\sim k_l$) between two neighboring atoms i and j sharing their valence electrons; a bending potential ($\sim k_\theta$) for all bond angles, including those in the phenyl rings; proper torsion and improper torsion potentials ($\sim k_\phi$). Coulomb interactions are not taken into account. For more details of the potential contributions and the values of all the potential constants we refer to [19,20].

In order to simulate supported aPS films, a completely smooth, structureless substrate is introduced at $z=0$ in the xy -plane of the simulation box of $70 \text{ \AA} \times 70 \text{ \AA}$. The periodic boundary conditions have

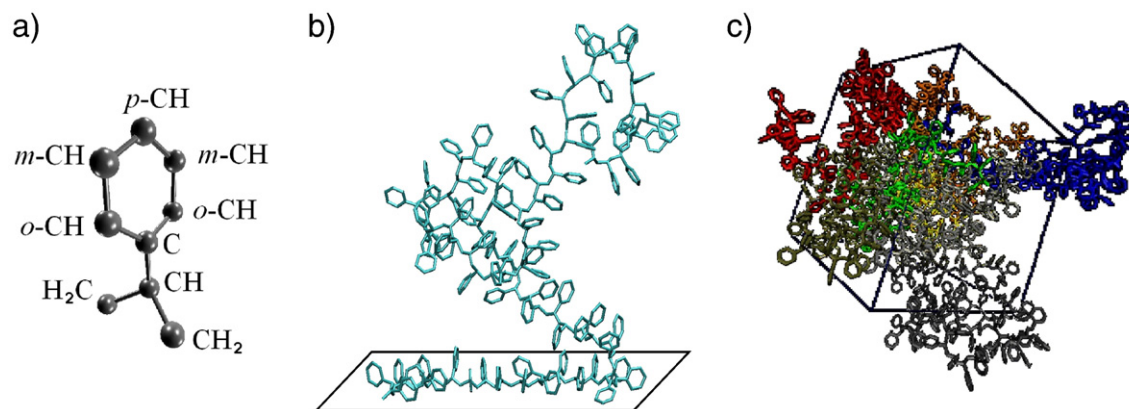


Fig. 1. a) aPS monomer with the naming convention of the united atoms. Here *o* = ortho, *m* = meta and *p* = para. b) Typical snapshot of one aPS chain in a many-chain supported film close to the substrate at $T = 540$ K. c) Simulated box (about $50 \text{ \AA} \times 50 \text{ \AA} \times 50 \text{ \AA}$) of 8 aPS chains in a bulk at $T = 540$ K.

been used only in the *xy*-plane of the film. To simulate the monomer-substrate interactions the following potential is chosen

$$U_{\text{sub}}(z) = \begin{cases} U_{\text{sub}}(z) - U_{\text{sub}}(R_{\text{cut}}), & z < R_{\text{cut}} \\ 0, & z > R_{\text{cut}} \end{cases} \quad (2)$$

$$U_{\text{sub}}(z) = \frac{1}{2} \varepsilon \left\{ \left(\frac{R_{\text{min}}}{z} \right)^9 - 3 \left(\frac{R_{\text{min}}}{z} \right)^3 \right\}.$$

Here in Eq. (2) ε is the strength of the attraction to the substrate and z denotes the distance from the monomer to the substrate. In the present simulations the attraction strength varies from $\varepsilon = 0.1$ kcal/mol to $\varepsilon = 3.0$ kcal/mol corresponding to both non-wetting and complete wetting conditions [21]. $R_{\text{min}} = 3 \text{ \AA}$ is the distance at the minimum of the potential and $R_{\text{cut}} = 9 \text{ \AA}$ is the cut-off distance. This potential mimics the van der Waals interactions between the atoms of the substrate and polymer segments, and can be obtained by integrating the 12-6 LJ potential over a half space [22]. The leap-frog velocity Verlet algorithm [23] has been used to integrate the Newtonian equations of motion with an integration time step of $\Delta t = 4$ fs. The Berendsen barostat [23] has been used, with time constant $\tau_p = 1$ ps. The temperature control has been performed using the collisional thermostat [24]. All MD simulations have been done with the help of modified PUMA MD program [24,25].

For both bulk and film geometries the simulated aPS box was allowed to relax for a sufficiently long-time (10 ns \div 20 ns), under a fixed external pressure (1 MPa \div 700 MPa). Each polymer system is equilibrated at an initial high temperature of 540 K in a high-mobility melt state. The quality of the equilibration was controlled by measuring the various statistical properties, such as the individual-chain radius of gyration, the chain end-to-end distance, and the characteristic ratio for different intermediate distances within each aPS chain. The external pressure was adjusted in order to reproduce the experimental bulk density of 0.914 g/cm^3 in the middle of the simulated film. For simulated bulk aPS the density was chosen a bit higher, close to 1 g/cm^3 .

After the equilibration the continuous cooling was performed with a constant cooling velocity of 0.01 K/ps down to the room temperature, 300 K, which is well below the known glass transition temperature (about 380 K) for this polymer. During the cooling procedure the aPS film trajectories have been saved every 20 K for a further analysis. Moreover, for each intermediate temperature, 1 ns MD film-production runs have been performed as well. About 50 ns run has been performed for an aPS bulk at $T = 300$ K to simulate the segmental mobility in a glassy state. In order to increase the statistics the simulations have been done for four independent aPS samples, in films or in a bulk.

In order to simulate the effects of the rejuvenation, a $50 \text{ \AA} \times 50 \text{ \AA} \times 50 \text{ \AA}$ box containing aPS bulk cooled down to $T = 300$ K is submitted to a cycle of uniaxial extension–compression. aPS samples

are stretched for about 30% (well above the yield point) and compressed back. Two deformation velocities, 0.001 \AA/ps (slow rejuvenation) and 0.05 \AA/ps (fast rejuvenation) have been used, corresponding to $2 \cdot 10^7 \text{ s}^{-1}$ and $1 \cdot 10^9 \text{ s}^{-1}$ strain rate, correspondingly.

3. Experimental details

Cyclic shear experiments on a glassy acrylate polymer were carried out using a lateral contact method. In this experiment, a crosslinked acrylate film (about 50 \mu m in thickness) is sheared within a circular macroscopic contact (about 660 \mu m in diameter) between a glass flat and a spherical glass lens under a constant applied normal load (30 N). By means of a piezo-electric actuator, small amplitude (between 0.15 \mu m and 5 \mu m) sinusoidal lateral displacements are imposed to the contact. During each loading cycle, the lateral force and displacement are continuously monitored in order to get the complex lateral contact stiffness defined as $K^* = F_t^*/\delta$, where F_t^* is the complex lateral force and δ is the displacement amplitude at the considered frequency (between 0.01 Hz and 8 Hz). Provided that the displacement is kept low enough (less than 5 \mu m), the film can be sheared without any significant micro-slip at the contact interface. In such a situation, the complex shear modulus of the film can be determined from the measured lateral contact stiffness both in the linear (viscoelastic) and in the non linear (plastic) range using a coated contact model developed within the limits of geometrically confined contacts (*i.e.* when the ratio of the contact radius to the film thickness is much larger than unity). Full details regarding the experimental methodology and data analysis are provided in references [18,26]. In addition to the complex shear modulus, nominal shear stress ($\tau = F_t/A$, where F_t is the lateral force and A is the contact area measured by optical observation) and strain ($\gamma = \delta/t$, where γ is the applied lateral displacement and t is the film thickness) can be measured.

The crosslinked acrylate film was obtained from the copolymerisation of *n*-butylmethacrylate (Acros Organics, purity 99%) and isobutylmethacrylate (Acros Organics, purity 99%) in a 1.2:1.0 molar ratio. A silane coupling agent was used in order to promote adhesion between the flat glass substrate and the film. Details on the realization of the films can be found in [26]. The glass transition temperature of the film is $52 \text{ }^\circ\text{C}$ as measured by Differential Scanning Calorimetry (DSC, $10 \text{ }^\circ\text{C/min}$). From the point of view of the performed MD simulations, it should be stressed that the acrylate film should be considered as a bulk system.

4. Effects of simulated mechanical rejuvenation on aPS bulk segmental dynamics

For initial, non-rejuvenated aPS samples the average density (black curve in Fig. 2b) is close to 1 g/cm^3 , and does not change much during the simulation (for the next ~ 50 ns). It means that the sample is already

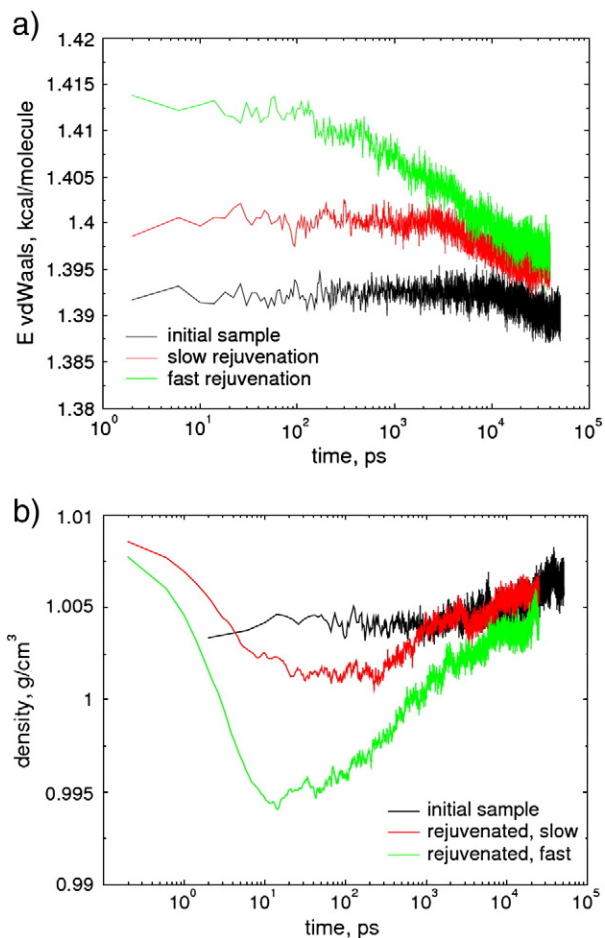


Fig. 2. Simulated changes of the aPS internal energy a) and density b) with time, for initial, non-rejuvenated (black curves) and rejuvenated polymer bulk at the end of the extension–compression cycle. $T = 300$ K.

aged enough. We can expect that the rejuvenation effects can be significant for such an old sample. After the rejuvenation cycle the total non-bonded (van der Waals) potential energy is definitely increased, as shown in Fig. 2a. Under the influence of the deformation the polymer chains are pulled out of local potential minima, to the new thermodynamic state, which lead to their closer packing and to some increase in excluded-volume interactions. It is also seen in the density plots, as shown in Fig. 2b. The immediate density after the deformation cycle is definitely higher as compared to that before the rejuvenation, the monomers are compressed. Immediately after the rejuvenation (up to 10 ps) the density starts to decrease, below the value of the initial samples, and larger free-volume holes are created. It is at least in qualitative agreement with the experimental findings [5,8]. At the same time no significant change in the non-bonded energy is observed. It means that this initial decrease in density takes place because of the fast relaxation of different (bending, stretching, and torsional) bonded energetic contributions. Then aging starts, the density starts to increase. Initially, with the onset of the aging, the non-bonded energy remains constant, this initial aging can be accounted for by the further relaxation of the bonded interactions. On a later stage (the slower the rejuvenation rate the later) the van der Waals energy starts to decrease, but with different rate for the samples rejuvenated with different deformation rate. Of course, aging takes place also for the non-rejuvenated samples, but for the rejuvenated samples the aging rate is much faster. The relative rate $\frac{1}{\tau} \frac{\Delta \rho}{\rho}$ where $\Delta \rho$ is the total change in density from minimum till maximum value during the time τ of the simulation is $4 \cdot 10^4 \text{ s}^{-1}$ for non-rejuvenated sample, and $2.4 \cdot 10^5 \text{ s}^{-1}$ and $4.4 \cdot 10^5 \text{ s}^{-1}$ for slowly

and faster rejuvenated samples, Fig. 2b, i.e. aging is increased drastically, about one order of magnitude.

The local orientational mobility in both non-rejuvenated and rejuvenated aPS bulk at $T = 300$ K has been studied with the help of Legendre polynomials of the second order (autocorrelation functions, ACFs)

$$P_2(t) = \langle 3/2(\mathbf{b}(0)\mathbf{b}(t))^2 - 1/2 \rangle, \quad (3)$$

where \mathbf{b} is the unit vector directed along the phenyl side group and the brackets denote the averaging over positions and over time, Fig. 3a. These vectors were analyzed separately at the ends and in the middle of each chain. Kohlrausch-Williams-Watts (KWW) [27] stretched exponential functions have been used to fit the final parts of the ACFs,

$$P_2(t) = \exp\left(-\left(t/\tau_2\right)^\beta\right), \quad (4)$$

where τ_2 is the characteristic orientational relaxation time and β is the parameter effectively taking into account the non-exponential nature of the relaxation process.

After the rejuvenation the local segmental mobility is changed. Rejuvenation drastically increases the relaxation rate, Fig. 3a, especially in the latest stage of the relaxation. The KWW fit cannot be used to describe the whole relaxation process, see Fig. 3b. It means that different relaxation mechanisms contribute differently to the

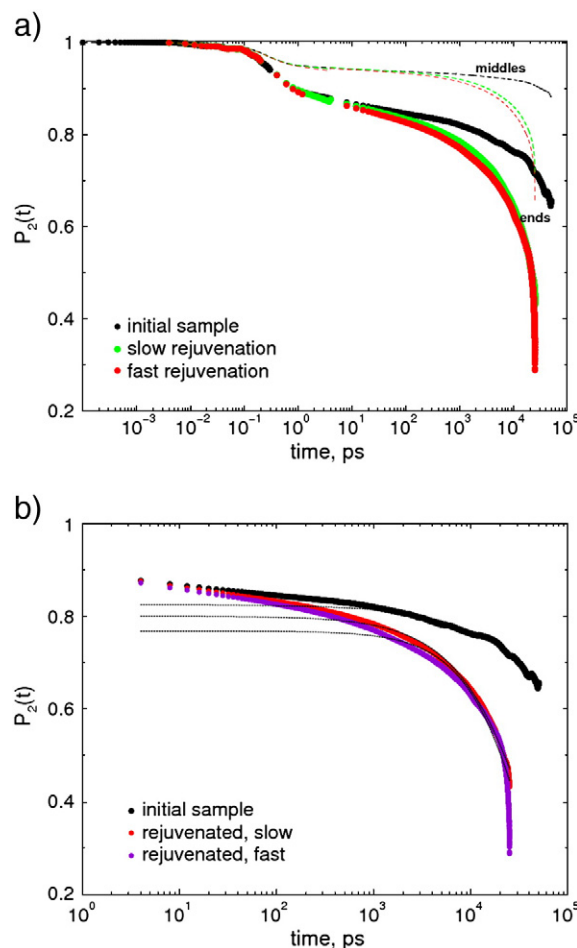


Fig. 3. a) Second order P_2 orientational autocorrelation functions for both initial and rejuvenated samples, for the phenyl group vectors at the ends and in the middle of the chain. b) KWW fits, Eq. (4) for both initial and rejuvenated samples for the phenyl group vectors at the ends of the chain.

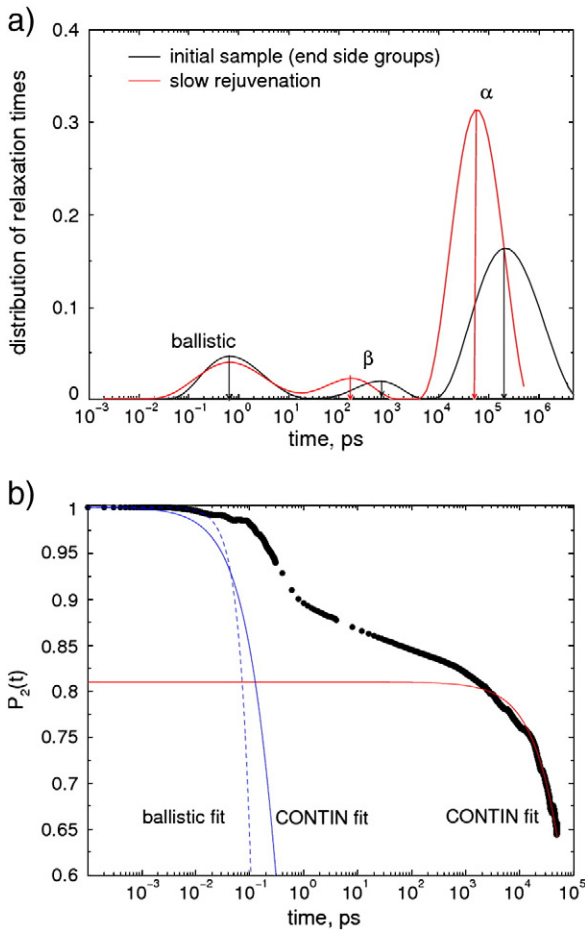


Fig. 4. a) Distribution function of the relaxation times for P_2 ACF of the average side bond vector at the chain ends for both initial and rejuvenated samples. b) Correspondent CONTIN fits for the P_2 ACF of the average side bond vector at the chain ends for initial sample.

orientational mobility. To take this into account, each ACF is also analyzed using the CONTIN [28] method

$$P_2(t) = \int_{-\infty}^{+\infty} F(\ln \tau) \exp(-t/\tau) d(\ln \tau), \quad (5)$$

where $F(\ln \tau)$ is a normalized distribution function of relaxation times.

The distribution function of the relaxation times is shown in Fig. 4a) for the end phenyl groups averaged over all aPS chains. Three relaxation processes are clearly seen. The magnitude of the long-time α process increases after the rejuvenation, and its position is clearly shifted to the shorter times. Ballistic process at very short times is not affected by the rejuvenation at all. Such a ballistic motion can describe only 1% of the total relaxation of the P_2 ACF (dashed line in Fig. 4b). The clear shift of the in-cage β relaxation takes place, also to shorter times. We noticed earlier that initially the density of the rejuvenated samples is higher as compared to the initial density for the aged polymer. The faster in-cage β relaxation is probably associated with this initial increase of the density. Finally, the increased aging rate after the rejuvenation is definitely explained by the faster α process for the rejuvenated material. We can take the positions of the CONTIN maxima, τ_i , and fit different parts of the ACF curves with single exponentials, $\exp(-t/\tau_i)$. Such a CONTIN fit works well, as shown in Fig. 4b.

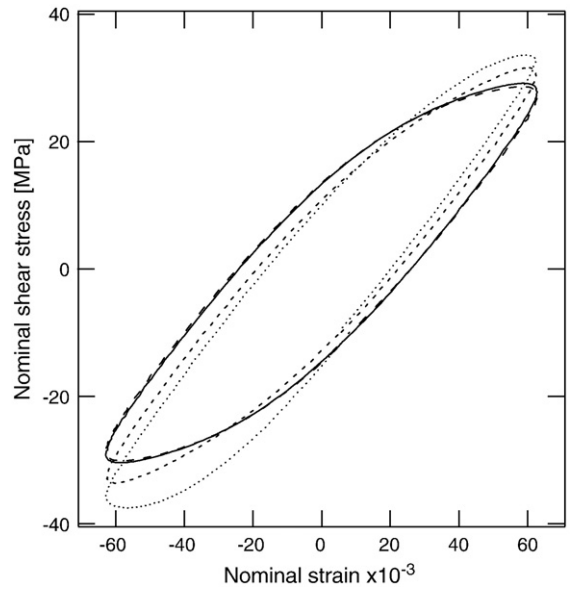


Fig. 5. Nominal stress–strain relationship during cyclic plastic deformation ($\gamma_0 = 6.4\%$, 1 Hz). Small dotted line: 2nd cycle; medium dotted line: 10th cycle, large dotted line: 50th cycle; and continuous line: 60th cycle.

5. Experimental results: cyclic shear experiments

Prior to the application of cyclic shear in the yield regime, the complex linear viscoelastic modulus, G^* , of the acrylate film is first measured in its reference state at low strain ($\gamma_0 = 0.5\%$) and for frequencies ranging from 0.05 to 10 Hz. No significant time dependent change in this modulus is observed after a contact time of more than 1 h, which means that physical aging processes of the virgin film are not detectable within this time frame. Sixty shear cycles at a large strain amplitude ($\gamma_0 = 6.4\%$) and at a frequency of 1 Hz are subsequently applied to the film in order to induce plastic deformation. During this stage, a time dependent shear response is observed: the nominal stress/strain relationship slowly evolves toward a steady state response characterized by a nearly elliptical cycle in a Lissajou representation (Fig. 5).

A strain and time dependent ‘apparent’ shear modulus, G_{app}^* can be ascribed to this non linear response which is determined from the in-phase and out-of-phase component of the lateral contact stiffness at the excitation frequency (1 Hz). In Fig. 6, the storage (G'_{app}) and dissipative (G''_{app}) components of this apparent shear modulus are reported as a function of the number of yield cycles. A strong drop in G'_{app} and a corresponding increase in G''_{app} are evidenced which presents some similarity with the large amplitude cyclic response of crosslinked epoxy

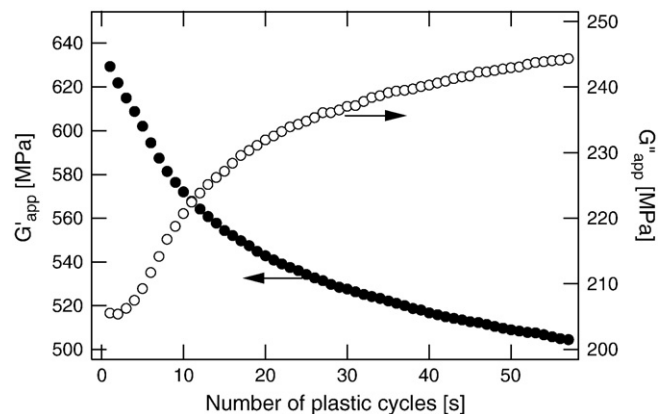


Fig. 6. Storage and loss components of the complex apparent modulus, (●) G'_{app} and (○) G''_{app} , as a function of the number of cycles in the plastic regime ($\gamma_0 = 6.4\%$, 1 Hz).

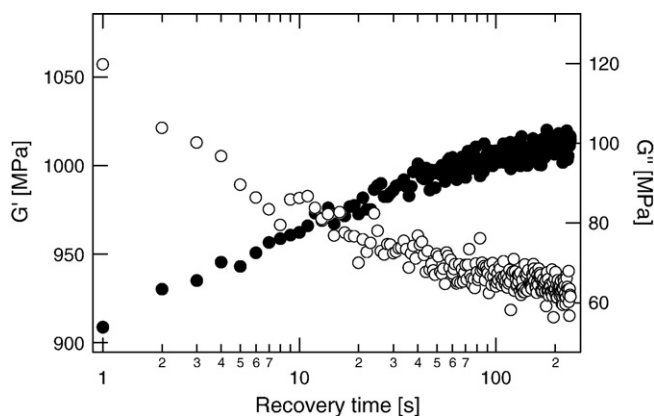


Fig. 7. Recovery of storage (G') and loss (G'') components of the linear viscoelastic modulus ($\gamma_0 = 0.5\%$, 1 Hz) after the application of 60 shear cycles in the yield regime ($\gamma_0 = 6.4\%$, 1 Hz). (●) G' ; (○) G'' . Before cyclic yield, the initial values of the components of the linear viscoelastic modulus are $G' = 1066 \pm 9$ MPa and $G'' = 67 \pm 3$ MPa.

resins in their glass transition zone [29]. Such changes in the apparent modulus may be viewed as evidence of an increased molecular mobility within the plastically deformed glass.

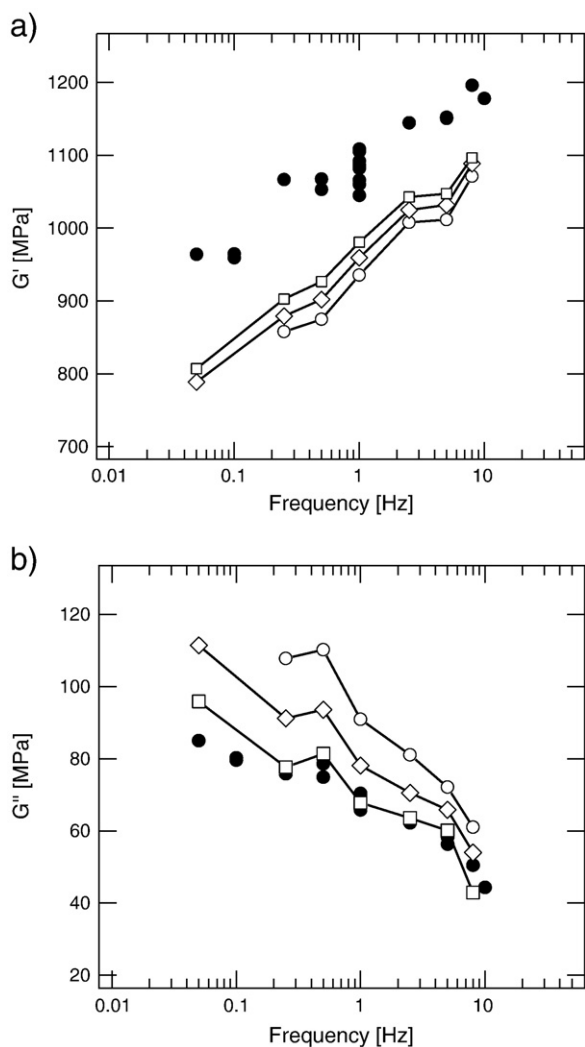


Fig. 8. Frequency dependence of (a) G' and (b) G'' at various times during a recovery step following 60 cycles in the plastic regime ($\gamma_0 = 6.4\%$, 1 Hz). (●) viscoelastic properties before yield; (○) $t = 4$ s, (◇) $t = 16$ s, and (□) $t = 128$ s after cyclic yield.

Further evidence of the changes in the dynamics of the yielded glass are provided from linear viscoelastic measurements at low strain ($\gamma_0 = 0.5\%$) carried out immediately after interruption of the large strain cycles. As compared to the initial (*i.e.* before yield) viscoelastic modulus ($G' = 1066 \pm 9$ MPa, $G'' = 67 \pm 3$ MPa), the storage modulus at 1 Hz is decreased by about 15% and the loss modulus is increased by about 80% immediately after cyclic yield (Fig. 7). However, a progressive recovery of these linear viscoelastic properties is observed as a function of time. Such a recovery may be viewed as evidence of enhanced physical aging rate of the mechanically rejuvenated glass (as mentioned above, no time dependent change in the linear viscoelastic properties of the virgin polymer was detected within the experimental time frame). After 240 s, only a partial recovery of G' was observed. Additional experiments with a longer recovery time (2000 s) did neither show a complete recovery of the storage modulus. However, when the film is heated above T_g (at about 70°C) and cooled down again, its initial viscoelastic properties are fully recovered which demonstrates that no permanent damage is involved in the observed changes in G^* after plastic deformation. The frequency dependence of the recovery was also examined. In Fig. 8, G' and G'' are reported as a function of frequency (between 0.1 and 8 Hz) after various recovery time. For the shorter recovery times, these spectra show a slight increase in the frequency dependence of the viscoelastic modulus of the yielded glass as compared to that of the virgin polymer, especially for the loss modulus G'' . Such increased frequency dependence may reflect the

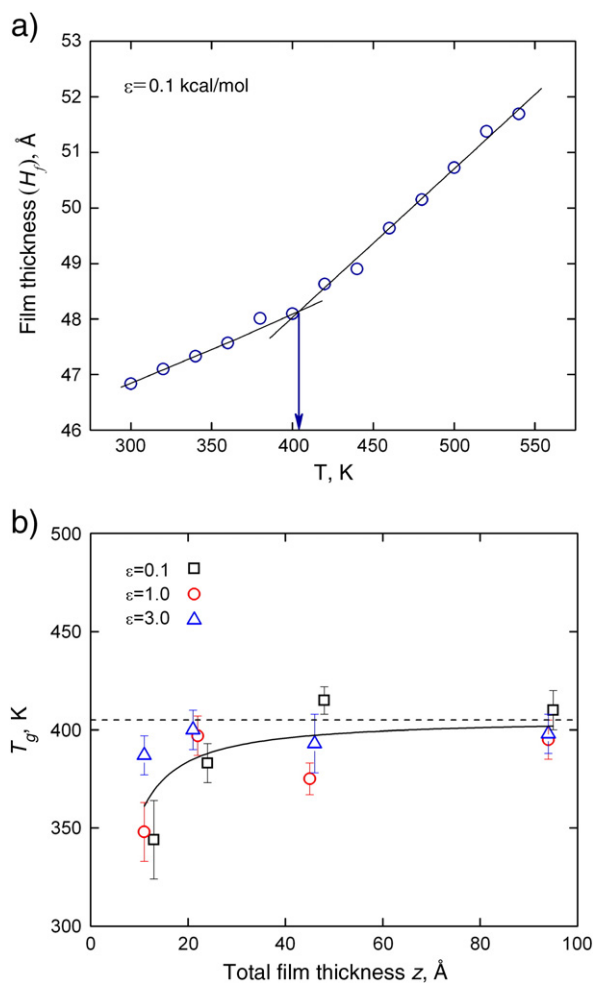


Fig. 9. Film thickness (a) as a function of temperature for aPS film with 16 chains in the case of a weak attraction ($\varepsilon = 0.1$ kcal/mol) to the substrate. Thickness dependence of T_g in a film for the case of weak (0.1 kcal/mol) and strong (1.0, 3.0 kcal/mol) attraction to the substrate. The dashed lines represent the simulated T_g value in the middle of the film. The solid line denotes the best fit to a data using the Eq. (6).

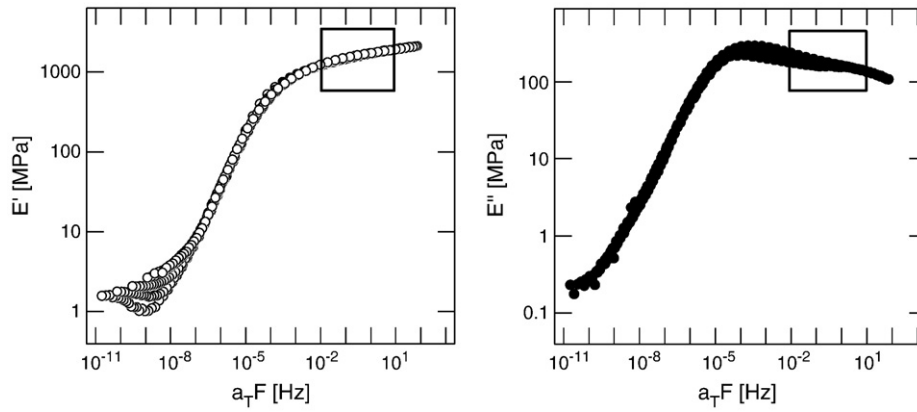


Fig. 10. Master curve giving the storage (E') and loss (E'') tensile modulus of the bulk acrylate as a function of frequency at 23 °C (from Dynamic Mechanical Thermal Analysis, D.M.T.A.). The boxes delimit the investigated frequency range during the recovery measurements.

fact that the polymer glass transition temperature is depressed after cyclic yield or, equivalently, that the relaxation times are shifted to shorter times. This point is further discussed in the discussion section.

6. Effects of simulated spatial confinement on aPS glass transition

We report here only very preliminary results on MD simulations of the glass transition in thin aPS films. Our nearest future plan is to apply the shear deformation to these films, and to see its effect on both glass transition and segmental polymer dynamics.

The glass transition temperature is measured by monitoring the temperature dependence of the film thickness (or density), selecting two linear regions of the data corresponding to high and low temperatures, fitting them by straight lines and finding the intersection point, as shown in Fig. 9a. Fig. 9b shows the thickness dependence of the T_g for the simulated aPS films. In this case, the T_g decrease with decreasing the aPS film thickness is observed, but only for very thin films, $z \leq 20 \text{ \AA}$. We fitted the simulation data in Fig. 9b by the empirical formula [30]:

$$T_g(z) = T_g^{bulk} \left(1 - \left(\frac{A}{z} \right)^\delta \right) \tag{6}$$

where T_g^{bulk} is the simulated T_g value in a middle of the film (indicated by the horizontal dashed line), the characteristic length $A = 1.8 \text{ \AA}$, the exponent $\delta = 1.1$, and z is the film thickness. These fitting results are quite different from the values which had been obtained by Keddie from the ellipsometry experiments ($A = 32 \pm 6 \text{ \AA}$, $\delta = 1.8 \pm 0.2$) [30], but are rather close to the results from the dielectric studies of Fukao ($A = 3.9 \pm 1.0 \text{ \AA}$, $\delta = 0.96 \pm 0.08$) [31]. We do not see any regular

dependence of the glass transition temperature on the strength of attraction to the substrate since the T_g values fluctuate considerably.

7. Discussion

Since the seminal work by Struik [1], experimental evidences have been accumulated to demonstrate that the application of large stresses or deformations results in an “erasure” of prior aging, or “rejuvenation” of polymer glasses. Such effects have been largely discussed from experiments where the mechanical response of the glass during or after a large deformation loading sequence is probed (creep compliance or relaxation modulus measurements). Some controversy regarding stress and volume relaxation phenomena induced by mechanical stimulation [2,32,33] especially led to the development of experimental methods where small incremental deformations are superposed on large deformations [1,34–36]. However, the analysis of such a non linear response is complicated by the potential superposition of two effects, namely (i) the change in glass dynamics resulting from stress induced structural changes, *i.e.* rejuvenation (ii) the “fading” memory effects emerging from the intrinsic non linear viscoelastic behavior of the polymer [33,37]. In the present study, the approach is different as the dynamics of the polymer glass *after* cyclic yield is probed in the linear viscoelastic range from complex shear modulus measurements carried out at a given frequency, which allows to discard the fading memory effects.

The time dependent viscoelastic spectra recorded immediately after cyclic yield are consistent with the occurrence of a mechanical “rejuvenation” effect. Accordingly G' is depressed and G'' is increased while an increased frequency dependence is observed. In Fig. 10, D.M.T.A. data for the bulk acrylate polymer are represented within an extended frequency range in the form of master curves at the reference temperature of 23 °C. In this figure, the boxed areas delimit the explored frequency

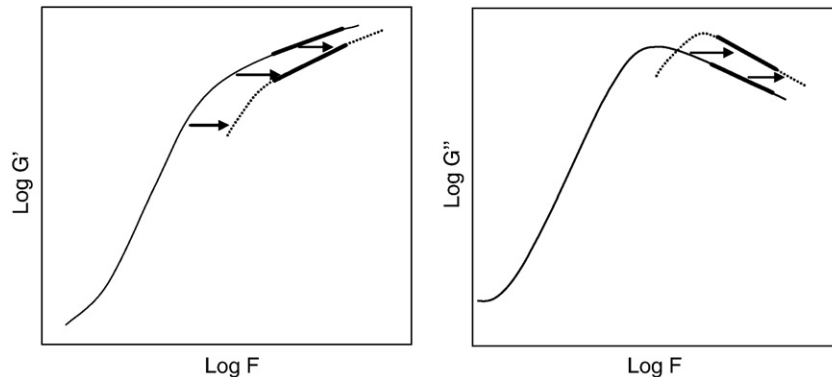


Fig. 11. Sketch depicting the assumed shift in the G' and G'' spectra after application of cyclic strain in the yield regime. Bold lines correspond to the frequency range probed experimentally.

range during the contact experiments which clearly lies in the sub- T_{α} region. From these data, one can speculate on the effects of a shift of the G^* spectra to high frequencies due to cyclic plastic deformation. As schematically depicted in Fig. 11, such a shift will result in a decrease (resp. increase) of G' (resp. G'') within the whole investigated frequency range, together with an increased frequency dependence. The observed changes in the shear linear viscoelastic modulus after cyclic yield are thus consistent with the hypothesis of a shift of the G' and G'' spectra to higher frequency or, in other words, to a shift of the relaxation spectra to shorter times.

8. Conclusion

We have performed molecular-dynamics simulations and a lateral contact experiment to investigate the influence of mechanical history on polymer mechanical behavior and segmental mobility. Cyclic shear strains applied in the plastic regime were found to induce a strong reduction of the apparent – non linear – shear modulus. Such a mechanical rejuvenation of the polymer is evidenced by a drop in the storage modulus and an increase in the loss modulus, as compared to the initial values recorded before plastic deformation. For the first time we connect this experimentally observed mechanical rejuvenation of polymer with the drastic increase in the simulated segmental mobility.

Although the timescales are completely different, the hypothesis of an experimental shift of the G' and G'' spectra to a higher frequency is supported by the MD simulations which show that the mechanical rejuvenation shifts the relaxation times distribution – both in α and β transition zones – to shorter times. As a result of the increased segmental mobility within the post-yield mechanically stimulated glass, aging is reinitiated as indicated by the progressive recovery of the viscoelastic properties. MD simulations results suggest that this recovery is associated with some structural recovery, as indicated by the time dependent increase in density.

We also observe the decrease of the glass transition temperature with polymer film thickness, but for extremely thin (less than 2 nm) films.

References

- [1] L.C.E. Struik, *Physical Aging in Amorphous Polymers and Other Materials*, Elsevier, Amsterdam, 1978.
- [2] G.B. McKenna, *J. Phys. Condens. Matter* 15 (2003) 737.
- [3] F.H. Stillinger, *Science* 267 (1995) 1935.
- [4] S.S. Jang, W.H. Jo, *J. Chem. Phys.* 110 (1999) 7524.
- [5] D. Cangialosi, M. Wübbenhorst, H. Schut, A. van Veen, S.J. Picken, *J. Chem. Phys.* 122 (2005) 064702.
- [6] L.J. Broutman, R.S. Patil, *Polym. Eng. Sci.* 11 (1971) 165.
- [7] L.J. Broutman, S.M. Krishnakumar, *Polym. Eng. Sci.* 14 (1974) 249.
- [8] H.G.H. van Melick, L.E. Govaert, B. Raas, W.J. Nauta, H.E.H. Mejer, *Polymer* 44 (2003) 1171.
- [9] O.A. Hasan, M.C. Boyce, *Polymer* 34 (1993) 5085.
- [10] F. Casas, C. Alba-Simionesco, H. Montes, F. Lequeux, *Macromolecules* 41 (2008) 860.
- [11] H.-N. Lee, K. Paeng, S.F. Swallen, M.D. Ediger, *Science* 323 (2009) 231.
- [12] F.M. Capaldi, M.C. Boyce, G.C. Rutledge, *Phys. Rev. Lett.* 89 (2002) 175505.
- [13] A.V. Lyulin, M.A.J. Michels, *Phys. Rev. Lett.* 99 (2007) 085504.
- [14] R.A. Riggleman, K.S. Schweizer, J.J. de Pablo, *Macromolecules* 41 (2008) 4969.
- [15] H.-N. Lee, R.A. Riggleman, J.J. de Pablo, M.D. Ediger, *Macromolecules* 42 (2009) 4328.
- [16] M. Warren, J. Rottler, *Phys. Rev. E* 78 (2008) 041502.
- [17] K. Van Workum, J.J. de Pablo, *Nanoletters* 3 (2005) 1405.
- [18] E. Gacoin, A. Chateauminois, C. Fretigny, *Tribol. Lett.* 21 (2006) 245.
- [19] A.V. Lyulin, N.K. Balabaev, M.A.J. Michels, *Macromolecules* 35 (2002) 9595.
- [20] B. Vorselaars, A.V. Lyulin, M.A.J. Michels, *Macromolecules* 40 (2007) 6001.
- [21] M. Müller, L.G. MacDowell, *J. Chem. Phys.* 118 (2002) 2929.
- [22] A.S. William, *The Interaction of Gases with Solid Surfaces*, London, Pergamon, 1974.
- [23] M.P. Allen, D.J. Tildesley, *Computer Simulation of Liquids*, Clarendon Press, Oxford, 1987.
- [24] A.S. Lemak, N.K. Balabaev, *Mol. Simul.* 15 (1995) 223.
- [25] A.S. Lemak, N.K. Balabaev, *J. Comput. Chem.* 17 (1996) 1685.
- [26] E. Gacoin, A. Chateauminois, C. Fretigny, *Polymer* 45 (2004) 3789.
- [27] G. Williams, D.C. Watts, *Trans. Faraday Soc.* 66 (1970) 80.
- [28] S. Provencher, *Comput. Phys. Commun.* 27 (1982) 213.
- [29] A.I. Isayev, D. Katz, Y. Smooha, *Polym. Eng. Sci.* 21 (1981) 566.
- [30] J.L. Keddie, R.A.L. Jones, *Faraday Discuss.* 98 (1994) 219.
- [31] K. Fukao, Y. Miyamoto, *Phys. Rev. E* 61 (2000) 1743.
- [32] L.C.E. Struik, *Polymer* 38 (1997) 4053.
- [33] W.K. Waldron, G.B. Mc Kenna, *J. Rheol.* 39 (1995) 471.
- [34] A.F. Yee, *J. Pol. Sci B: Pol. Phys.* 26 (1988) 2463.
- [35] G.B. Mc Kenna, L.J. Zapas, *J. Pol. Sci. B: Pol. Phys.* 23 (1985) 1647.
- [36] S. Yoshioka, H. Usada, Y. Nanzai, *J. Non Cryst. Sol.* 172–174 (1994) 765.
- [37] L. Grassia, A. D'Amore, *Phys. Rev. E* 74 (2006) 021504.